Optics Letters

High-efficiency supercontinuum generation in solid thin plates at 0.1 TW level

Peng He,[1,2] Yangyang Liu,[2] Kun Zhao,[2,*] Hao Teng,[2] Xinkui He,[2] Pei Huang,[3] Hangdong Huang,[1] Shiyang Zhong,[2] Yujiao Jiang,[1] Shaobo Fang,[2] Xun Hou,[3] and Zhiyi Wei[2,4]

[1]School of Physics and Optoelectronics Engineering, Xidian University, Xi'an 710071, China
[2]Beijing National Laboratory for Condensed Matter Physics, Institute of Physics, Chinese Academy of Sciences, Beijing 100190, China
[3]Xi'an Institute of Optics and Precision Mechanics, Chinese Academy of Sciences, Xi'an 710119, China
[4]e-mail: zywei@iphy.ac.cn
*Corresponding author: zhaokun@iphy.ac.cn

Received 12 October 2016; revised 24 November 2016; accepted 2 January 2017; posted 3 January 2017 (Doc. ID 278550); published 24 January 2017

Supercontinuum generation in a solid-state medium was investigated experimentally. A continuum covering 460 to 950 nm was obtained when 0.8 mJ/30 fs Ti:sapphire laser pulses were applied to seven thin fused silica plates at a 1 kHz repetition rate. The primary processes responsible for spectral broadening were self-phase modulation (SPM) and self-steepening, while SPM and self-focusing were balanced to optimize the spectral broadening and suppress the multiphoton process. The output was compressed to a 5.4 fs and a 0.68 mJ pulse, corresponding to two optical cycles and 0.13 TW of peak power.

OCIS codes: (320.6629) Supercontinuum generation; (190.7110) Ultrafast nonlinear optics; (320.7100) Ultrafast measurements.

https://doi.org/10.1364/OL.42.000474

Attosecond optics is among the most celebrated offspring of atomic, molecular, and optical physics. Its essence is the generation of isolated attosecond optical pulses through high-order harmonic generation (HHG) and the investigation of electronic motion on an atomic scale with such pulses [1,2]. One of the key issues is that the photon flux in an attosecond pulse is extremely low. Although extreme ultraviolet (XUV) pulses as short as 67 as have been demonstrated [3], a typical isolated attosecond pulse contains only about 1 nJ of energy [4,5], which is not strong enough to carry out autocorrelation, nonlinear optics, or multiphoton process experiments. Generally speaking, 1 μJ of pulse energy is required to study nonlinear atto-optics. Such an energetic pulse will be able to exploit the full potential of all-attosecond studies and open new research fields.

Considering the conversion efficiency of about 10^{-5} to 10^{-7} for HHG and attosecond pulse generation [4,6], one way to produce a 1 μJ attosecond pulse is to drive the generation process with a 1 J femtosecond pulse. Although an XUV pulse as short as 148 as [7], an XUV continuum with about 100 nJ [8], and a 500 as pulse with over 1 μJ energy [9] generated by multi-cycle driver pulses have great potential to raise the pulse energy further, few- or mono-cycle driving pulses would certainly be much more efficient, since an isolated attosecond pulse is actually produced within only a half-cycle of the driver [10]. Boosting the energy of such a short pulse involves generating and/or amplifying a spectrum covering an octave or more, which is rather challenging at a joule energy level due to the gain narrowing effect in chirped pulse amplification [8].

Supercontinuum generation (SCG) by self-phase modulation (SPM) [11,12] of narrow-band driving pulses has been investigated since the laser was invented [13], implementing broadband light sources for a variety of applications [14]. A coherent octave or broader spectrum may be utilized to produce few- to mono-cycle optical pulses. Currently, the mainstream technique of few-cycle pulse generation is to compress multi-cycle pulses from laser amplifiers with inert-gas-filled hollow-core fibers (HCFs), plus the chirped mirrors which deliver pulses of 1 to 3 cycles [15,16]. However, such a device only takes pulses with energy on the order of millijoules, and the transmission is usually only ~50%, hardly over 70%. The primary energy loss mechanism includes multiphoton processes (absorption or ionization) and waveguide mode selection. This technique faces considerable challenges to accommodate more powerful input pulses. The highest pulse energy attempted so far was 75 mJ at an 800 nm central wavelength [17] and 11 mJ at 1.8 μm [16], while the output was only 10.9 mJ and 5 mJ, respectively. At the same time, HCF compressors suffer other technical complications, including a rather large footprint, poor long-term stability, delicate construction, and tedious alignment for daily operation.

Spectral broadening in solid-state materials has been presented [13] and pursued as a pulse compression technique [18–23] which, however, did not yield octave-spanning spectra. Lately, a supercontinuum similar to that from HCFs has been generated from bulk dielectrics [24,25], and mid-infrared few-cycle pulses have been obtained [22,23,26–28]. In addition to SPM which induces the desired SCG, the optical Kerr effect also triggers undesired self-focusing. With that, the laser beam shrinks, and the intensity raises drastically, causing significant multiphoton excitation and ionization, which lead to serious energy loss and permanent damage to the material if the pulse energy is high enough [29,30]. The pulse energy of the supercontinuum from solid-state materials is so far limited to the order of 100 μJ, except in [23], where the broadened spectrum with 20 mJ of energy did not reach an octave.

Several papers [18,19,31] have mentioned using a short slab of dielectrics to minimize the effect of self-focusing—the beam exits the medium before it starts to damage. However, a slab does not provide enough nonlinearity for SCG. To avoid catastrophic self-focusing while generating a supercontinuum, using multiple Kerr elements has been proposed [32,33] and demonstrated experimentally at a sub-millijoule level [25]. In the proposal [32], a periodic system was considered to achieve spectrum broadening, consisting of a thin piece of Kerr medium and a relay telescope in each element. At higher intensities, self-focusing in even a very thin solid-state plate could make a positive lens, so that each plate itself could act as one element to achieve spectrum broadening periodically. In such a system, a femtosecond laser pulse may be spectrally broadened via SPM through each plate, while self-focusing in the same medium produces a converging beam only after propagating through. Once the converging beam passes its minimal cross section (focal spot), it becomes diverging again and enters the next plate.

Utilizing this configuration, consisting of multiple fused silica plates, we generated an octave-spanning supercontinuum. With input pulses of 0.8 mJ/30 fs at 1 kHz, 0.7 and 0.68 mJ pulses were obtained after the plates and chirped mirrors, corresponding to efficiencies of 87.5% and 85%, respectively. The center spot of the beam (Fig. 2), containing 85% of the pulse energy, gave a 74% efficiency after the plates by itself. The output spectrum supported a transformed-limited pulse duration of 3.5 fs. A compressed pulse duration of 5.4 fs at full width at half-maximum was measured by a home-built transient-grating frequency-resolved optical gating (TG-FROG) [34]. This corresponds to a two-cycle 0.13 TW pulse and, to the best of our knowledge, was the first millijoule pulse approaching the terawatt level with an octave spectrum produced by SPM in solid-state material. Compared with HCFs, SCG in multiple thin plates is a promising way to obtain few-cycle pulses with the advantages of high efficiency, good stability, and a compact footprint. More importantly, this scheme would allow generation of few-cycle pulses with much higher energy and at different central wavelengths.

The experimental apparatus for SCG in fused silica plates and pulse compression is schematically illustrated in Fig. 1. Driving pulses of 0.8 mJ and 30 fs with a central wavelength at 790 nm were produced at 1 kHz by a multi-pass Ti:sapphire amplifier. A telescope and a lens were used to control the diameter and divergence of the beam. Without the plates, the beam diameter was $2w_0 = 600$ μm (at $1/e^2$ of the intensity profile) at the focal point, the Rayleigh range was $z_R = 35$ cm, and the intensity was about 9.4×10^{12} W/cm^2. The beam propagated through seven pieces of fused silica, each of which was 0.1 mm thick and 10 mm in diameter, placed at the Brewster's angle (55.5°), giving an effective thickness 0.12 mm.

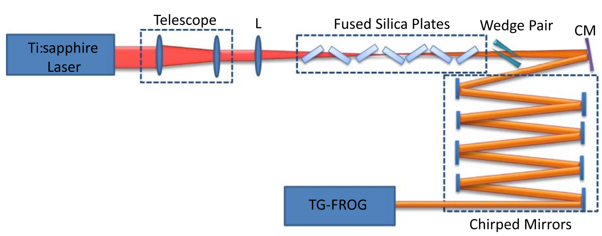

Fig. 1. Experimental setup for supercontinuum generation in fused silica plates and pulse compression. The telescope contained two fused silica lenses, a plano–convex with $f = 300$ mm and a plano–concave with $f = -100$ mm separated by 200 mm; the focusing lens (L) was $f = 2000$ mm. CM, concave silver mirror, to collimate the output beam ($f = 1000$ mm). The chirped mirrors were from FEMTOLASERS (part# BBCOMP).

The major nonlinear optical process contributing to SCG was the Kerr effect, which caused SPM, as well as self-focusing [11,29,35]. At higher laser intensities ($\gtrsim 10^{14}$ W/cm^2), ionization-enhanced SPM (IE-SPM) [36–38] may be invoked to explain the strong spectral broadening to the short-wavelength side [17,39]. Although IE-SPM results in a broader spectrum, the ionization causes substantial energy loss. Therefore, we chose to focus loosely and optimized the locations of the plates for best SPM to obtain a spectrum as broad as possible, while limiting the effect of self-focusing, and thus ionization, to minimize energy loss.

The first plate was 31 cm before the focus of the 2 m lens for optimal SCG and a compact optical path [21,40], and the beam diameter was about 0.8 mm before the plate. The diameter right after the plate reduced to 0.45 mm, and kept decreasing to a minimum of roughly 0.4 mm. The second plate was located 20 cm behind the first one, and the beam diameter at the plate was measured as 0.4 mm. The distances from the plate in front for the remaining five plates were 8.5 cm, 4.5 cm, 5 cm, 5 cm, and 5 cm, respectively, so that the total distance from the first to the last one was about 50 cm. Each plate was placed behind the minimal beam size produced by the plate in front, and self-focusing in each plate changed a slightly diverging incident beam into a slightly converging one. The beam diameters were the same at the third and fourth ones, and increased to 0.5 mm, 0.6 mm, and 0.8 mm for the fifth to seventh plates, respectively. The laser intensities were about 2.1×10^{13} W/cm^2 in the first four plates, and dropped to 5.3×10^{12} W/cm^2 in the last one, assuming a constant pulse width of 30 fs. The final output had M^2 of 1.86 and 1.69 in two orthogonal axes, while the input had 1.68 and 1.34, measured by a beam analyzer (M2-200s-FW, Spiricon). The output power stability was 0.45% (rms over 50 min), measured by a power meter with an integration time of 100 ms (PM2/LabMax, Coherent), while the input was 0.63%.

The seven thin plates, each of which acted as the nonlinear medium for SCG, as well as a relay lens to confine the beam [32], assembled a quasi-periodic quasi-waveguide to broaden the spectrum continually. In this configuration, on the one hand, the beam size was kept more or less the same within 50 cm by self-focusing through the plates to maximize SPM. On the other hand, the beam had left the plate every time self-focusing made the beam converging so that the beam would not be focused inside the plate to cause damage. After passing through all the plates, the beam at far field, as shown in the inset of Fig. 2, had a high-quality transverse mode similar to that of a HCF output, which took the form of a zeroth-order Bessel function [15]. The final spectrum was shown in Fig. 2, covering an octave from 460 to 950 nm at a −20 dB intensity level, which supported a transform-limited pulse duration of 3.5 fs. The spectra of the center peak and the first ring, which together contained over 95% of the energy, were essentially the same. The output energy was 0.70 mJ, corresponding to an efficiency of 87.5%. This result and the efficiency of 74% for the center spot were much higher than HCFs, which are usually

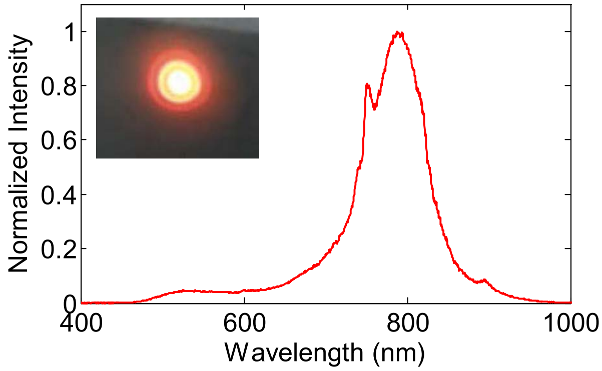

Fig. 2. Supercontinuum after the laser beam propagated through seven fused silica thin plates. Inset: the output beam profile taken at the collimating mirror; the center peak was saturated to show the structures of the rings.

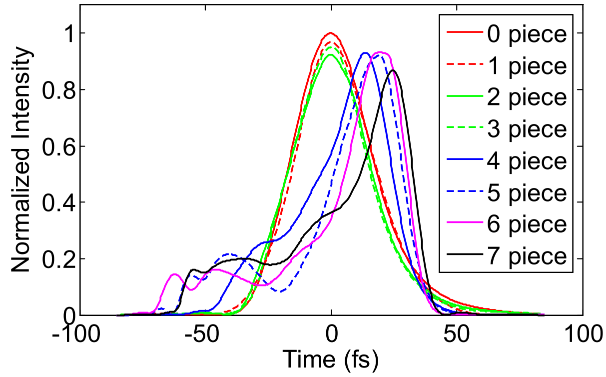

Fig. 4. Pulse envelopes retrieved from FROG traces taken after each fused silica plate. The zeroth one was the input. The energy of each pulse was normalized to the input.

~50% for the full beam, and higher than previous similar studies [25]. The efficiency of each plate increased gradually from 95% to 99.3% from the first to the last. By adjusting the parameters of the telescope and focusing lens, a similar output mode and spectrum were obtained with input pulse energy between 0.2 and 0.8 mJ. The total efficiency increased from 87.5% to 90%, as the input energy decreased from 0.8 to 0.2 mJ. The observed higher efficiencies at later thin plates where the beam diameter was getting larger, as well as at lower input energies, indicated that a lower energy loss was correlated with lower laser intensity and, thus, weaker multiphoton processes.

To understand how the laser pulse evolved through the plates, the spectrum and pulse shape after each plate were measured experimentally. The spectra in a log scale were shown in Fig. 3, while the intensity temporal profiles obtained by FROG in Fig. 4. As shown in Fig. 3, the spectral broadening in the first three plates was more or less symmetric to the pump spectrum, and the corresponding pulse shapes in Fig. 4 were also symmetric and did not change. This was typical SPM which broadened the spectrum, but did not modify the temporal envelope. However, at the fourth plate, self-steepening set in, and a sharp edge started to appear on the tail of the pulse (the blue solid curve in Fig. 4). As the pulse passed through the remaining plates, the self-steepening was strengthened—a steep trailing edge became more pronounced, and a broad short-wavelength pedestal appeared in the spectra (blue dashed, purple, and black curves in Figs. 3 and 4). Adding more plates did not change the spectrum further.

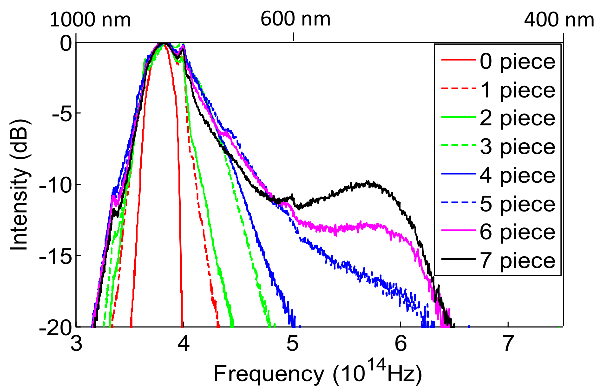

Fig. 3. Spectra taken after each fused silica plate in a log scale. The zeroth one was the input spectrum.

In a Kerr medium, the refractive index is $n = n_0 + n_2 I$, where n_0 is the linear refractive index, n_2 is the nonlinear refractive index coefficient, and I is the laser intensity [41]. In space, the intensity peaks at the center of the beam so as n for regular material ($n_2 > 0$), which manifests itself as self-focusing. While the beam collapse in the medium caused by self-focusing had to be circumvented by using thin plates, it was self-focusing that kept the beam size more or less the same throughout all the plates. The observation that the beam diameter increased from 0.4 to 0.6 mm in 23 cm (from the second to sixth plates), while the Rayleigh range of a 0.4 mm diameter beam was only 15.7 cm, was an indication of the beam confining effect in our setup. In the time domain, the intensity variation produces a phase modulation, $\phi(t) = \frac{2\pi n_0 L}{\lambda} + \frac{2\pi n_2 I(t) L}{\lambda}$, which exhibits a frequency shift in the spectral domain, $\Delta\omega = -\frac{\partial}{\partial t}\phi(t) = -\frac{2\pi n_2 L}{\lambda}\frac{\partial I(t)}{\partial t}$, where L is the length of the nonlinear medium and λ the central wavelength [41]. Meanwhile, seeing a higher n, the intensity peak takes a lower group velocity and moves toward the trailing edge—self-steepening, which causes excess spectral broadening on the short-wavelength side. Our observation (Fig. 4) showed qualitative consistency with previous studies, where SPM and self-steepening were considered as the primary nonlinear optical processes in SCG [11,35]. Self-steepening reduced the peak width, but due to a large pedestal at the leading edge and energy loss at each plate, the peak dropped as well (Fig. 4). Therefore, the self-focusing was also reduced, and the beam size increased significantly at the last two plates, causing the intensity to drop further and, eventually, the spectral broadening stopped.

The output beam was collimated by a concave mirror then four pairs of chirped mirrors and a pair of fused silica wedges were employed to compensate and control the chirp (Fig. 1). A pulse width of 5.4 fs (Fig. 5) was measured by a home-built TG-FROG [34]. The pulse energy measured after the chirped mirrors and wedges was 0.68 mJ, while the center spot contained 0.58 mJ.

In conclusion, we investigated SCG in solid-state media in order to develop high-energy femtosecond laser pulses to drive high-energy isolated attosecond pulses. Utilizing seven fused silica thin plates as the nonlinear medium, with input pulses of 0.8 mJ/30 fs at 1 kHz, an octave-spanning spectrum supporting a transformed-limited pulse duration of 3.5 fs was obtained. The pulse energy after the plates and compressor were 0.7 and 0.68 mJ, corresponding to the efficiencies of 87.5% and 85%, respectively. A compressed pulse width of 5.4 fs was

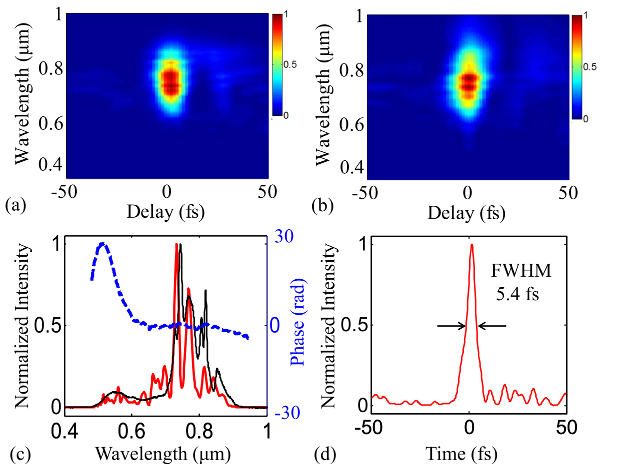

Fig. 5. Characterization of the 5.4 fs pulse compressed from the supercontinuum by TG-FROG. (a), (b) Measured and reconstructed FROG traces. (c) Retrieved spectrum (solid red line), phase (dashed line), and the spectrum taken at the entrance of the FROG (solid black line). (d) Retrieved pulse envelope. The retrieval error was 0.008.

measured by a TG-FROG, representing a two-cycle 0.13 TW pulse. The center spot, containing 85% of the pulse energy or 0.58 mJ after compression, corresponded to 0.11 TW itself. To the best of our knowledge, this was the first millijoule pulses approaching the terawatt level with an octave-spanning spectrum produced by SPM in solid-state materials.

The primary processes in the SCG were SPM and self-steepening. While self-focusing was restricted to suppress the catastrophic effect of strong focusing in bulk materials by using thin plates, it was utilized to maintain a quasi-waveguide, where the plates were the quasi-periodic elements to confine the beam so as to maintain effective spectral broadening. Therefore, SPM and self-focusing, the two leading nonlinear processes, were successfully balanced to optimize the SCG while suppressing the multiphoton process, which was the major energy loss mechanism. The achieved efficiency was much higher than mainstream HCF systems (50%) and previous similar experiments.

Compared with HCFs, SCG in multiple plates was not only efficient, but also stable, robust, and reproducible on a more compact footprint. Our setup had been producing the same spectrum continuously for over 6 h without any manual alignment or automated beam pointing stabilization system, and the spectrum had stayed unchanged for several days when the laser was switched on and off every day. This scheme should be applicable to a wide range of lasers with spectra covering ultraviolet to mid-infrared, and scalable to much higher pulse energies, although the inhomogeneity and instability on the wavefront may trigger small-scale self-focusing and, eventually, set an upper limit of the applicable pulse energy. The development of high-power few- to mono-cycle laser sources is invaluable, not only for high-energy attosecond pulse generation, but for many nonlinear optics, ultrafast optics, and strong field physics applications, and will open new research areas that have been previously inaccessible.

Funding. National Key Basic Research Program of China (2013CB922401, 2013CB922402); National Natural Science Foundation of China (NSFC) (11434016, 11574384, 61575219); International Joint Research Program of the National Natural Science Foundation of China (61210017).

REFERENCES

1. M. Chini, K. Zhao, and Z. Chang, Nat. Photonics **8**, 178 (2014).
2. L.-Y. Peng, W.-C. Jiang, J.-W. Geng, W.-H. Xiong, and Q. Gong, Phys. Rep. **575**, 1 (2015).
3. K. Zhao, Q. Zhang, M. Chini, Y. Wu, X. Wang, and Z. Chang, Opt. Lett. **37**, 3891 (2012).
4. H. Mashiko, S. Gilbertson, C. Li, E. Moon, and Z. Chang, Phys. Rev. A **77**, 063423 (2008).
5. F. Ferrari, F. Calegari, M. Lucchini, C. Vozzi, S. Stagira, G. Sansone, and M. Nisoli, Nat. Photonics **4**, 875 (2010).
6. I. J. Kim, C. M. Kim, H. T. Kim, G. H. Lee, Y. S. Lee, J. Y. Park, D. J. Cho, and C. H. Nam, Phys. Rev. Lett. **94**, 243901 (2005).
7. X. Feng, S. Gilbertson, H. Mashiko, H. Wang, S. D. Khan, M. Chini, Y. Wu, K. Zhao, and Z. Chang, Phys. Rev. Lett. **103**, 183901 (2009).
8. Y. Wu, E. Cunningham, H. Zang, J. Li, M. Chini, X. Wang, Y. Wang, K. Zhao, and Z. Chang, Appl. Phys. Lett. **102**, 201104 (2013).
9. E. J. Takahashi, P. Lan, O. D. Mücke, Y. Nabekawa, and K. Midorikawa, Nat. Commun. **4**, 2691 (2013).
10. P. B. Corkum, N. H. Burnett, and M. Y. Ivanov, Opt. Lett. **19**, 1870 (1994).
11. G. Yang and Y. R. Shen, Opt. Lett. **9**, 510 (1984).
12. R. R. Alfano, ed., *The Supercontinuum Laser Source*, 3rd ed. (Springer, 2016)
13. F. Shimizu, Phys. Rev. Lett. **19**, 1097 (1967).
14. T. Brabec and F. Krausz, Rev. Mod. Phys. **72**, 545 (2000).
15. M. Nisoli, S. De Silvestri, and O. Svelto, Appl. Phys. Lett. **68**, 2793 (1996).
16. V. Cardin, N. Thiré, S. Beaulieu, V. Wanie, F. Légaré, and B. E. Schmidt, Appl. Phys. Lett. **107**, 181101 (2015).
17. O. Hort, A. Dubrouil, A. Cabasse, S. Petit, E. Mével, D. Descamps, and E. Constant, J. Opt. Soc. Am. B **32**, 1055 (2015).
18. C. Rolland and P. B. Corkum, J. Opt. Soc. Am. B **5**, 641 (1988).
19. V. Petrov, W. Rudolph, and B. Wilhelmi, J. Mod. Opt. **36**, 587 (1989).
20. D. H. Reitze, A. M. Weiner, and D. E. Leaird, Opt. Lett. **16**, 1409 (1991).
21. E. Mével, O. Tcherbakoff, F. Salin, and E. Constant, J. Opt. Soc. Am. B **20**, 105 (2003).
22. M. Hemmer, M. Baudisch, A. Thai, A. Couairon, and J. Biegert, Opt. Express **21**, 28095 (2013).
23. V. Shumakova, P. Malevich, S. Ališauskas, A. Voronin, A. M. Zheltikov, D. Faccio, D. Kartashov, A. Baltuška, and A. Pugžlys, Nat. Commun. **7**, 12877 (2016).
24. M. Bradler, P. Baum, and E. Riedle, Appl. Phys. B **97**, 561 (2009).
25. C.-H. Lu, Y.-J. Tsou, H.-Y. Chen, B.-H. Chen, Y.-C. Cheng, S.-D. Yang, M.-C. Chen, C.-C. Hsu, and A. H. Kung, Optica **1**, 400 (2014).
26. F. Silva, D. Austin, A. Thai, M. Baudisch, M. Hemmer, D. Faccio, A. Couairon, and J. Biegert, Nat. Commun. **3**, 807 (2012).
27. A. A. Lanin, A. A. Voronin, E. A. Stepanov, A. B. Fedotov, and A. M. Zheltikov, Opt. Lett. **40**, 974 (2015).
28. H. Liang, P. Krogen, R. Grynko, O. Novak, C.-L. Chang, G. J. Stein, D. Weerawarne, B. Shim, F. X. Kärtner, and K.-H. Hong, Opt. Lett. **40**, 1069 (2015).
29. A. L. Gaeta, Phys. Rev. Lett. **84**, 3582 (2000).
30. A. Couairon and A. Mysyrowicz, Phys. Rep. **441**, 47 (2007).
31. N. Krebs, I. Pugliesi, and E. Riedle, Appl. Sci. **3**, 153 (2013).
32. S. Vlasov, E. Koposova, and V. Yashin, Quantum Electron. **42**, 989 (2012).
33. A. A. Voronin, A. M. Zheltikov, T. Ditmire, B. Rus, and G. Korn, Opt. Commun. **291**, 299 (2013).
34. J. N. Sweetser, D. N. Fittinghoff, and R. Trebino, Opt. Lett. **22**, 519 (1997).
35. J. E. Rothenberg, Opt. Lett. **17**, 1340 (1992).
36. G. Tempea and T. Brabec, Opt. Lett. **23**, 1286 (1998).
37. A. Brodeur and S. L. Chin, Phys. Rev. Lett. **80**, 4406 (1998).
38. A. Brodeur and S. L. Chin, J. Opt. Soc. Am. B **16**, 637 (1999).
39. C. Fourcade Dutin, A. Dubrouil, S. Petit, E. Mével, E. Constant, and D. Descamps, Opt. Lett. **35**, 253 (2010).
40. D. Wang, D. X. Li, X. W. Chen, Y. X. Leng, and Z. Z. Xu, Laser Phys. **20**, 1410 (2010).
41. A. Siegman, *Lasers* (University Science Books, 1986), Chap. 10.